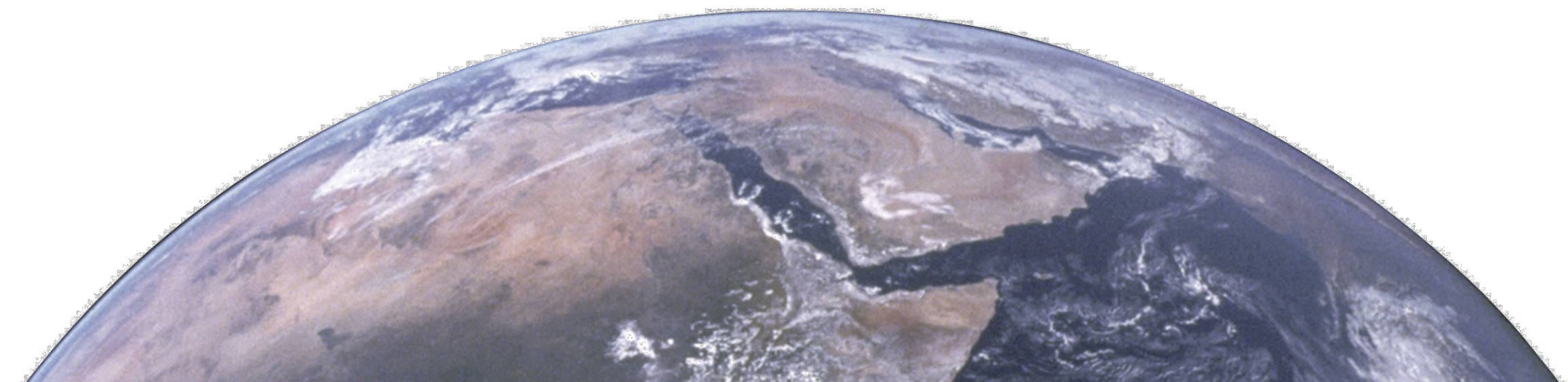


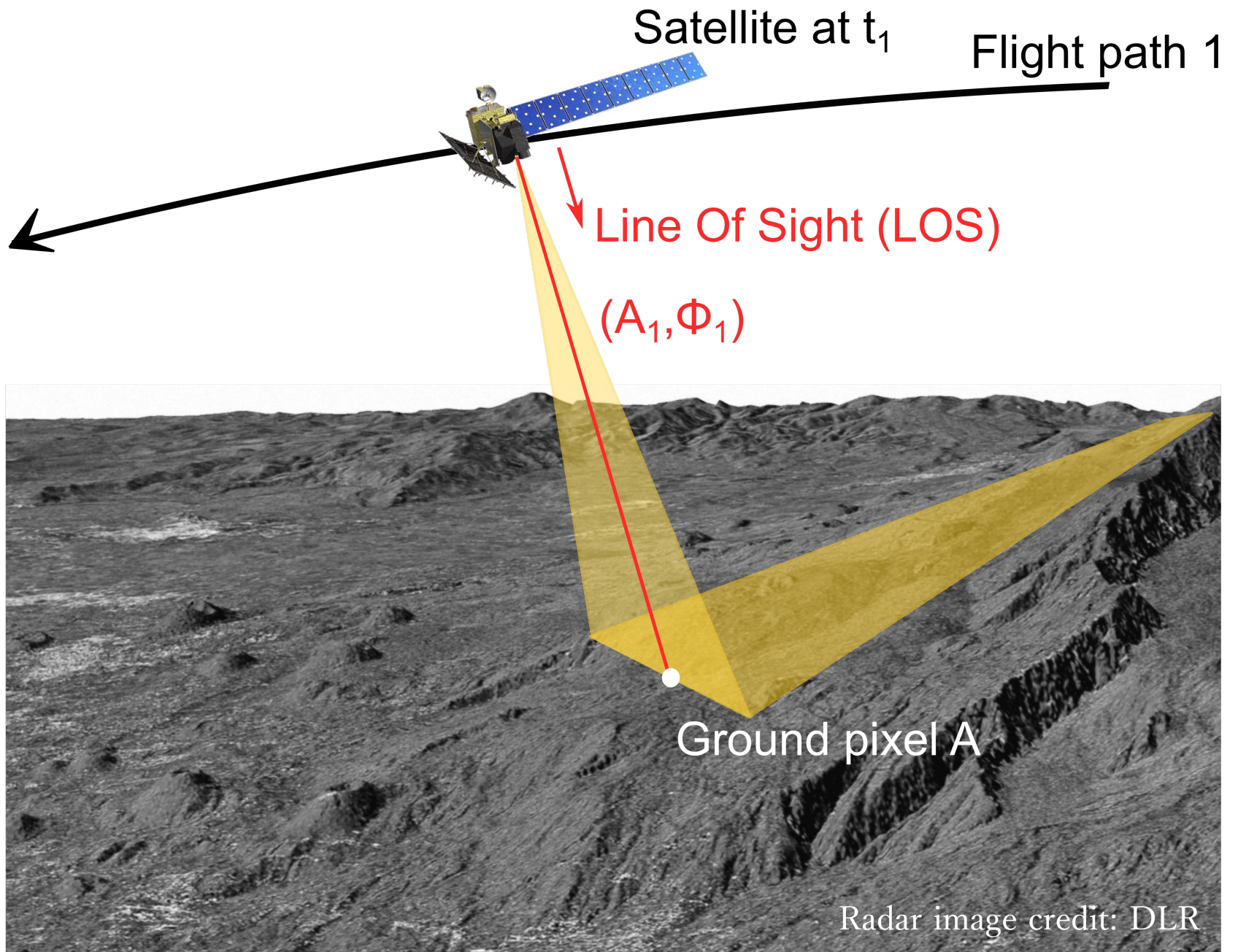
# Imaging Radar data interpretation and analysis for Earth Science Studies

Ann Chen

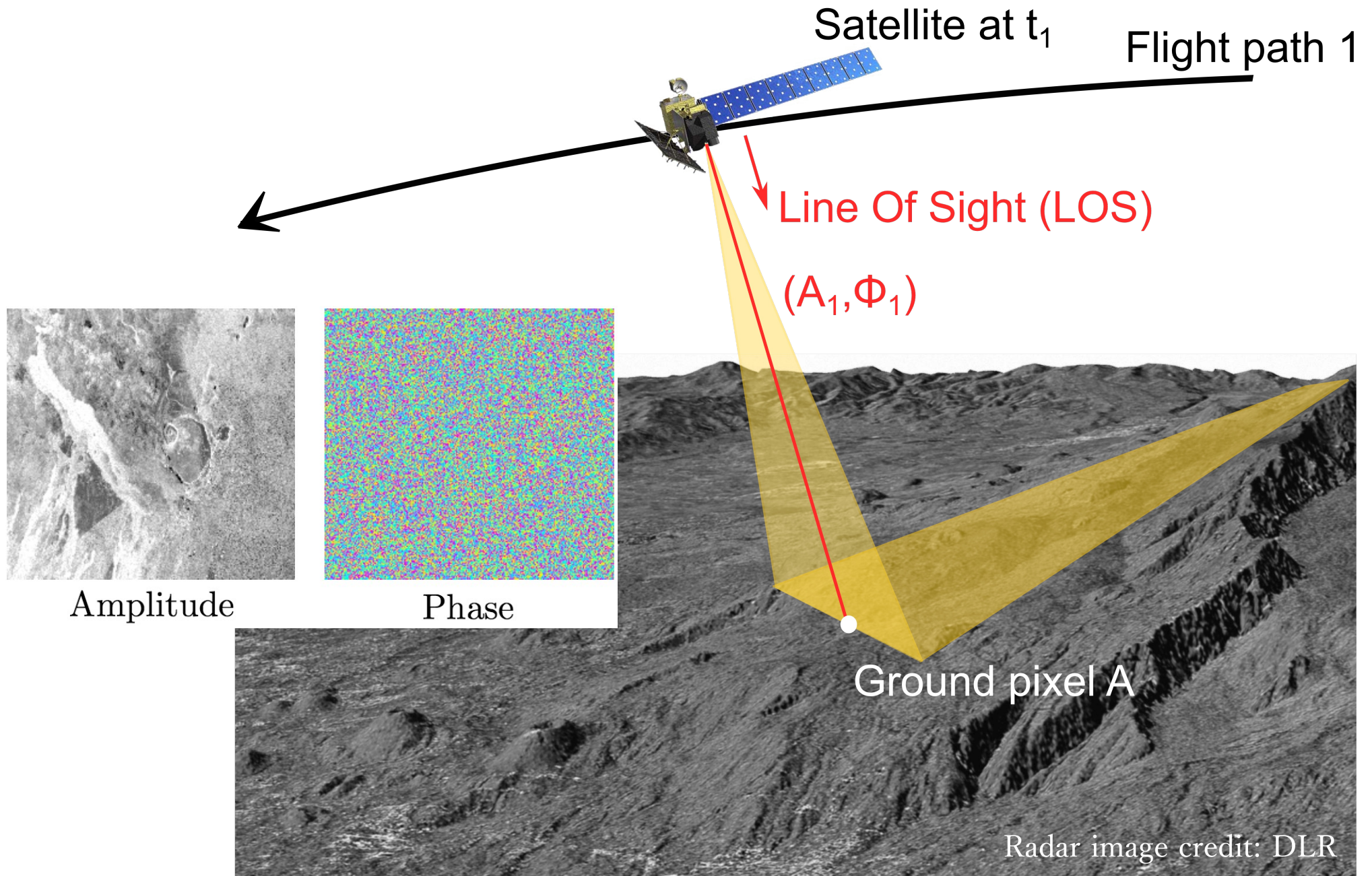
Department of Aerospace Engineering and  
Engineering Mechanics, the University of Texas  
at Austin



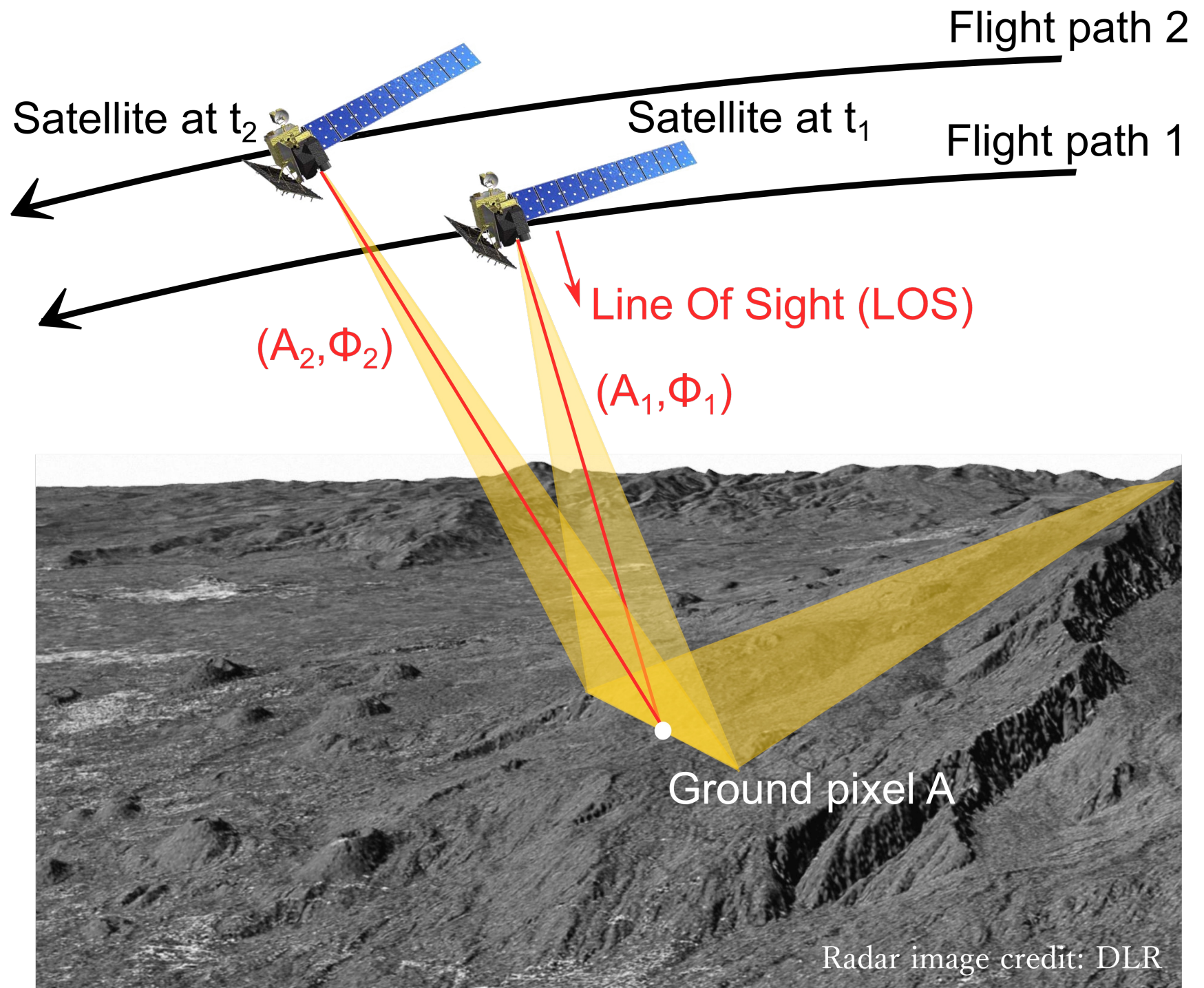
# Synthetic Aperture Radar



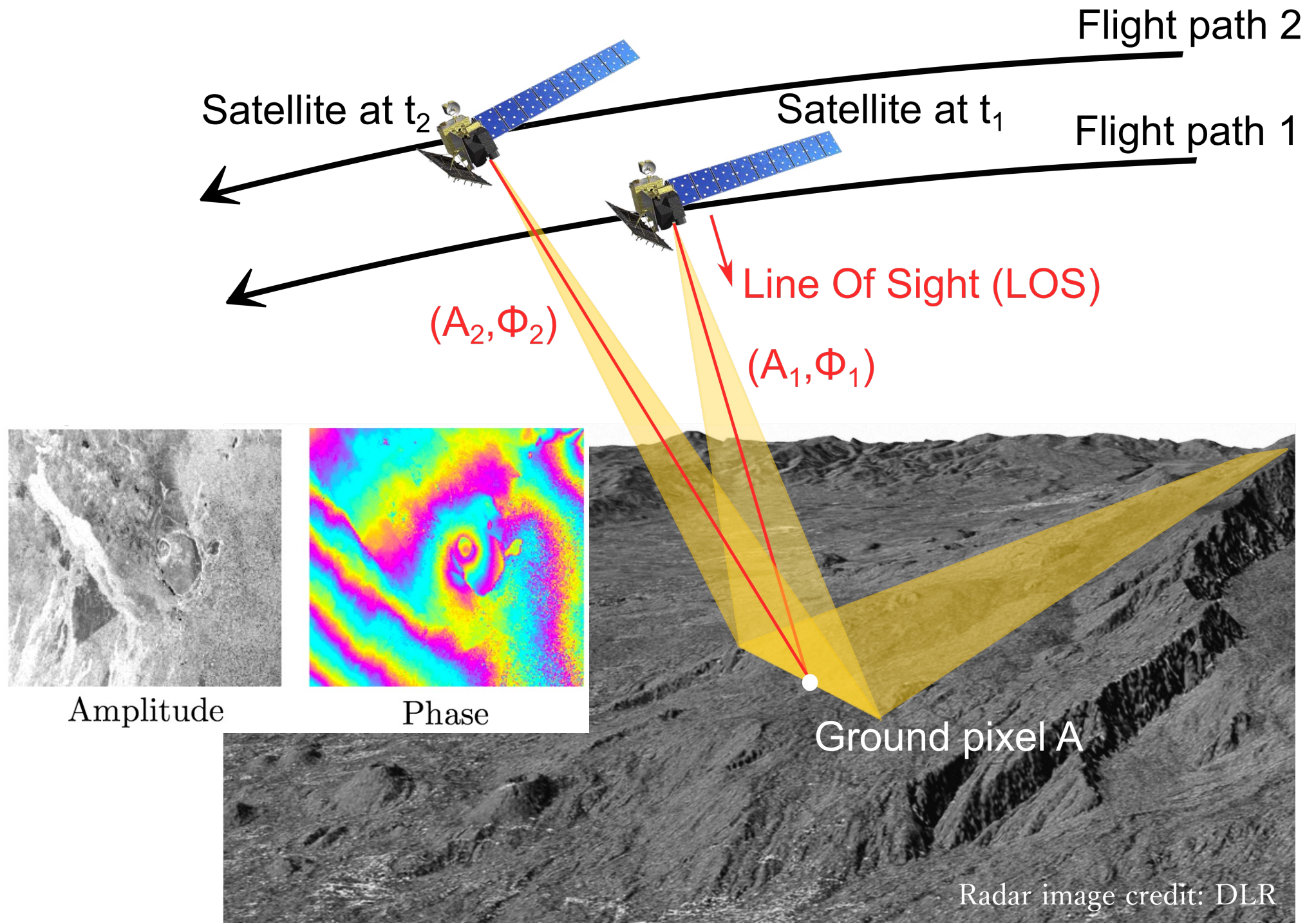
# Synthetic Aperture Radar



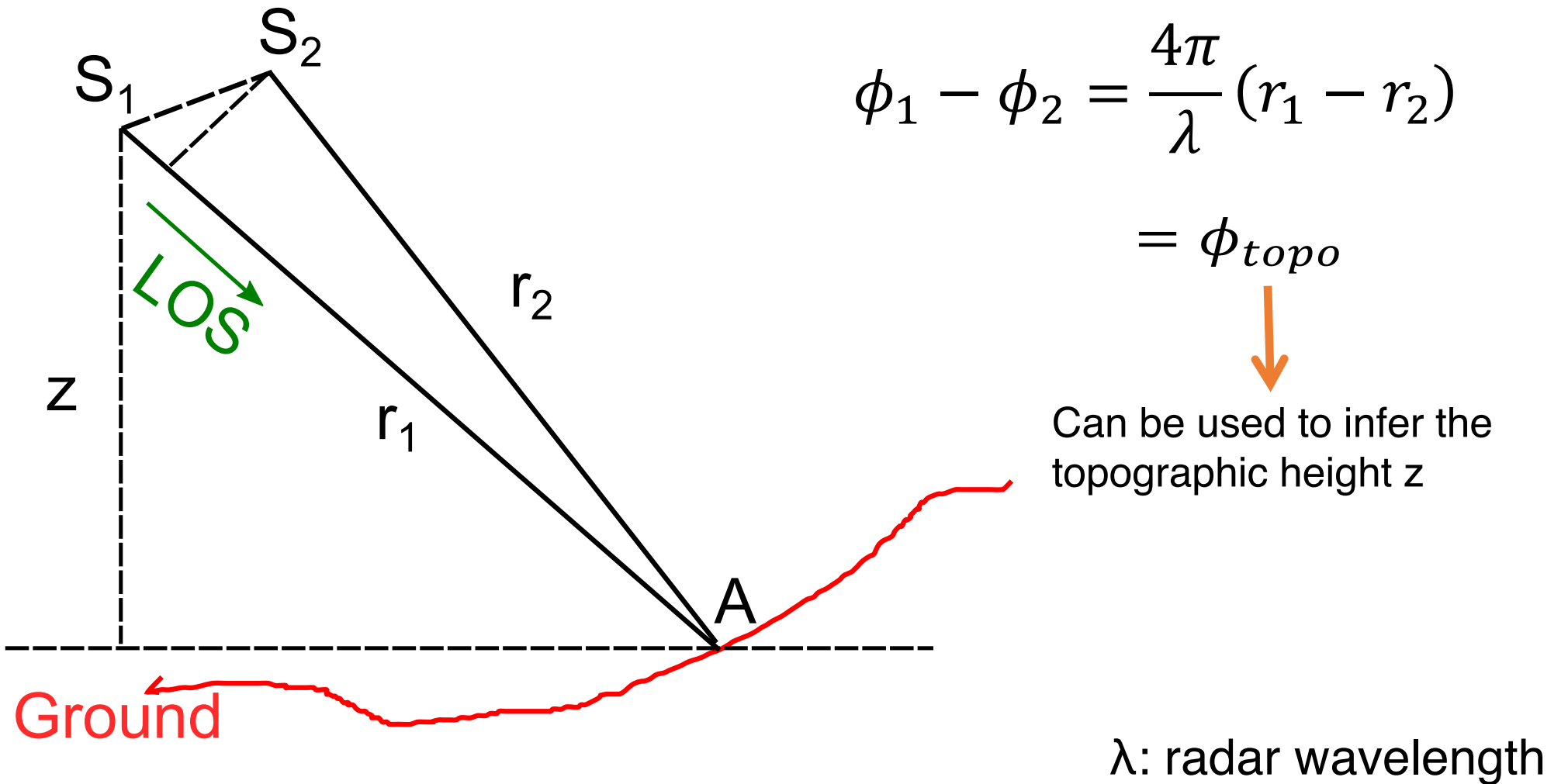
# Interferometric Synthetic Aperture Radar



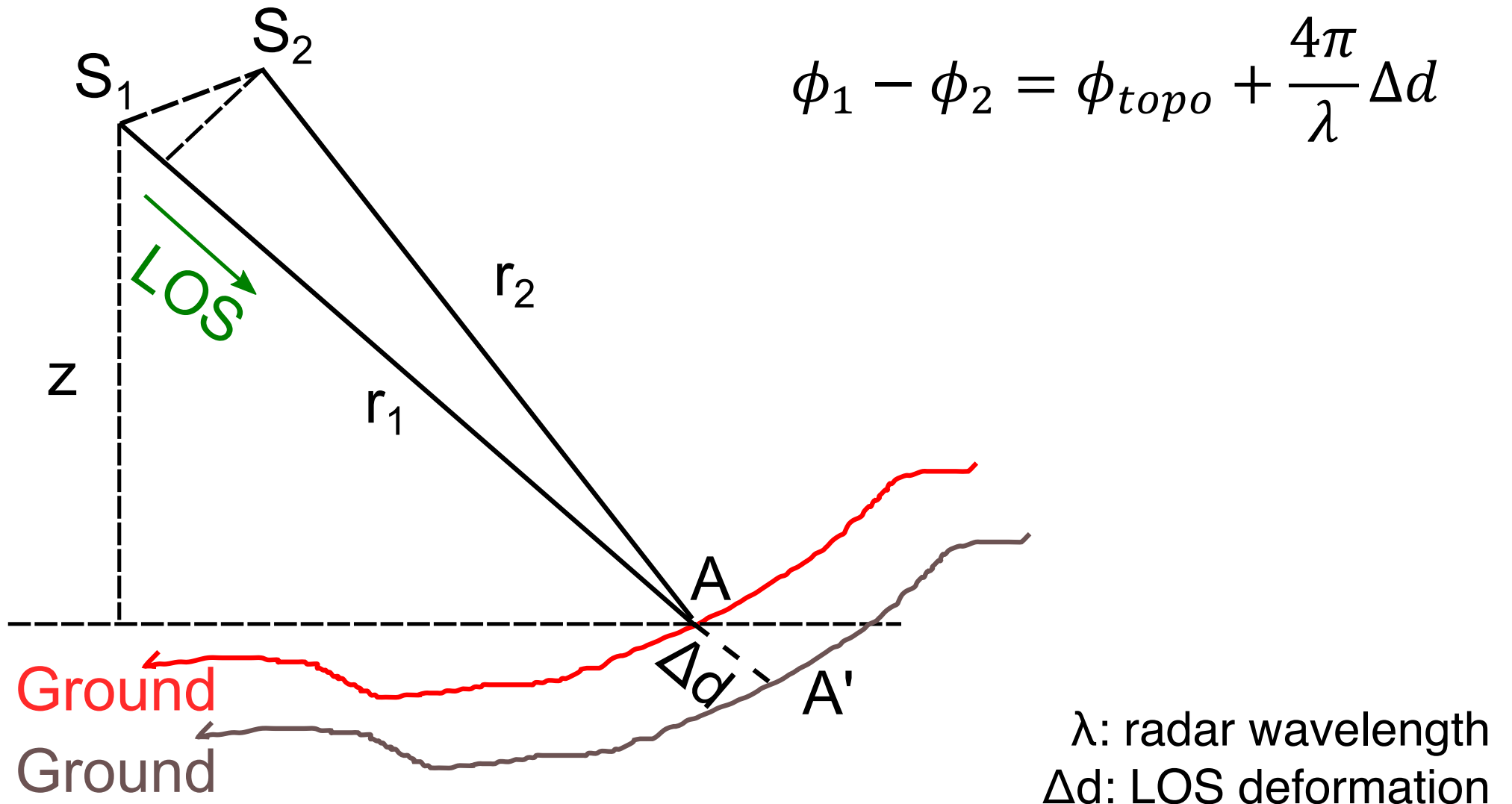
# Interferometric Synthetic Aperture Radar



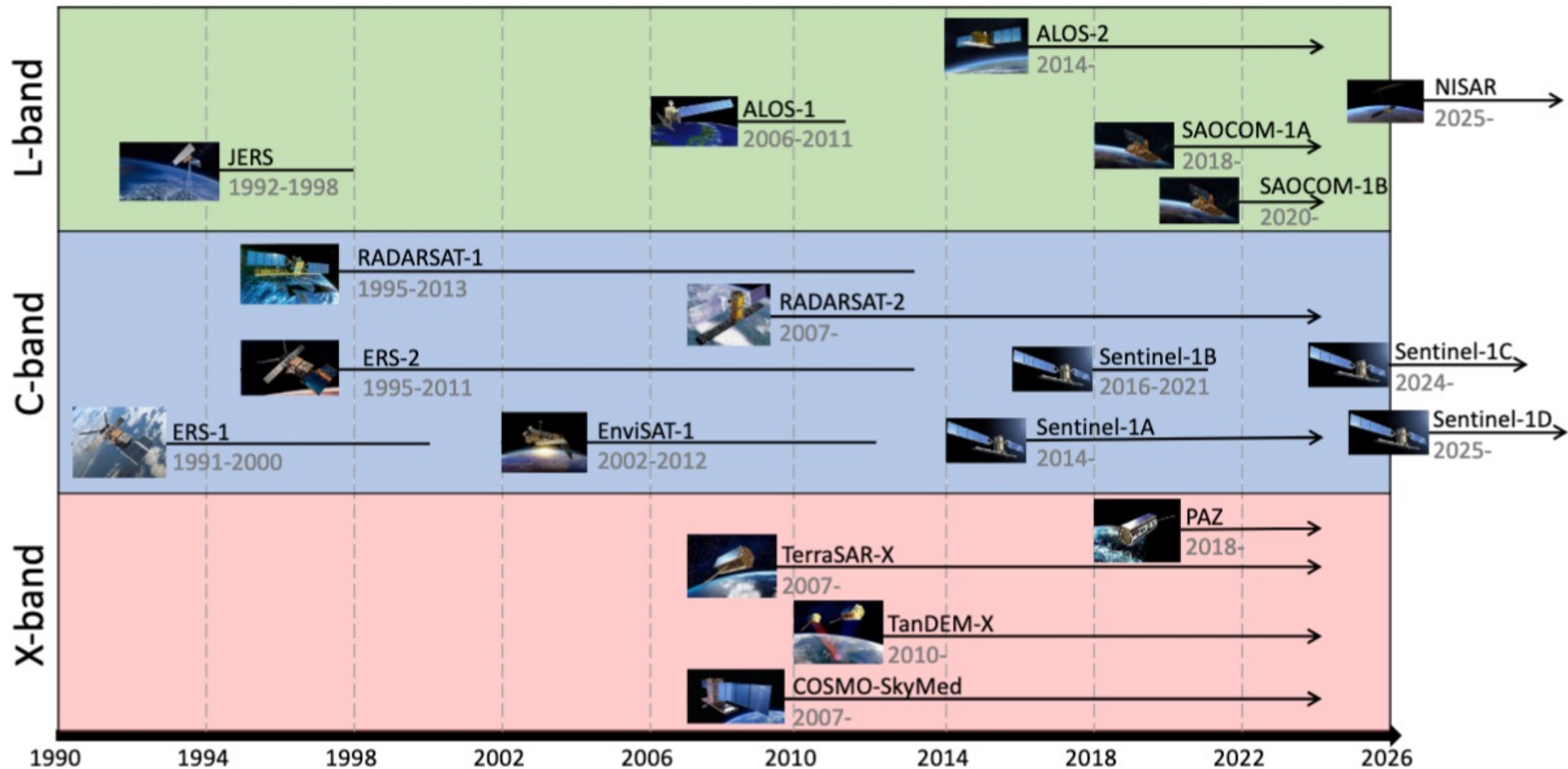
# InSAR acquisition geometry



# InSAR acquisition geometry



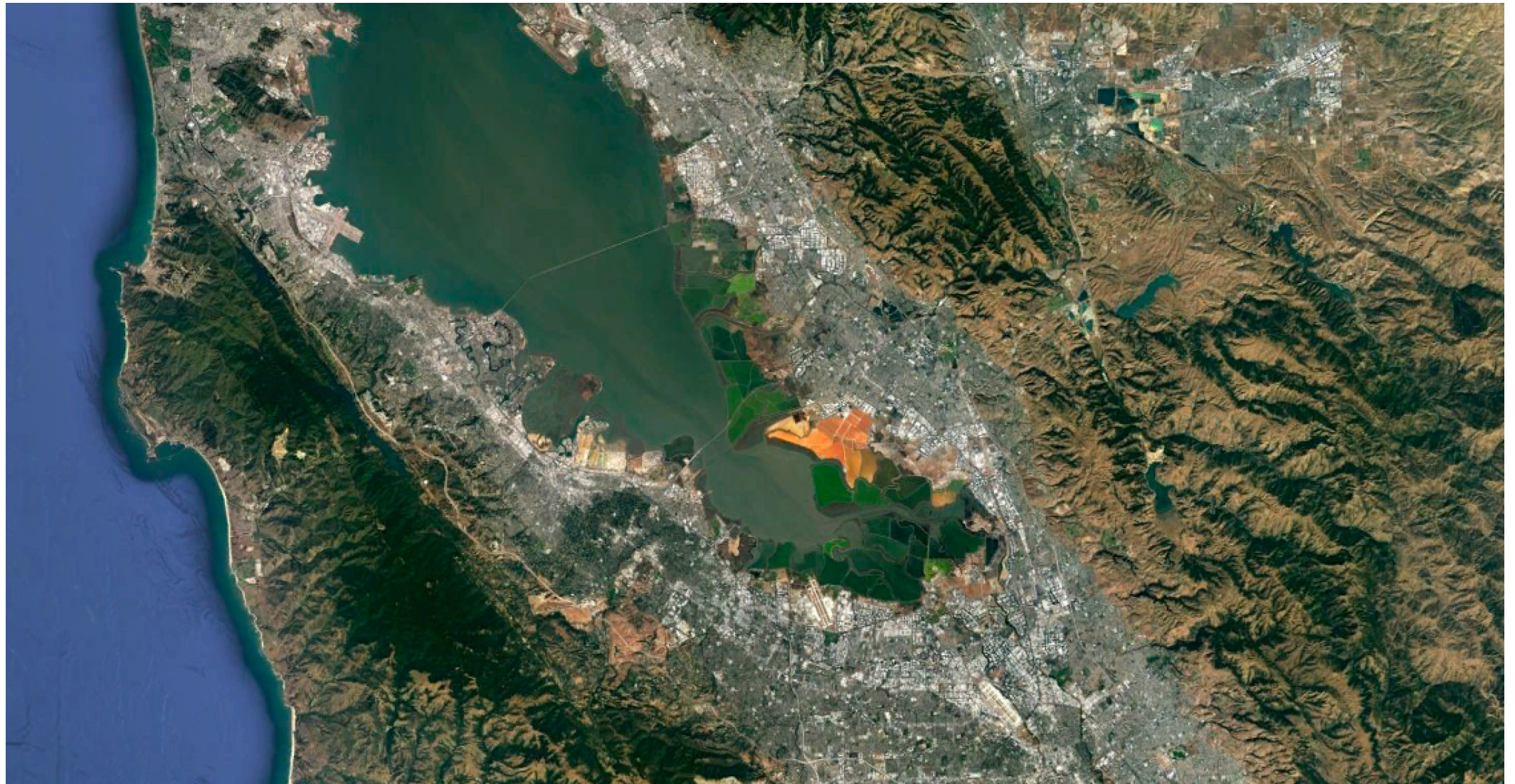
# Available spaceborne InSAR missions



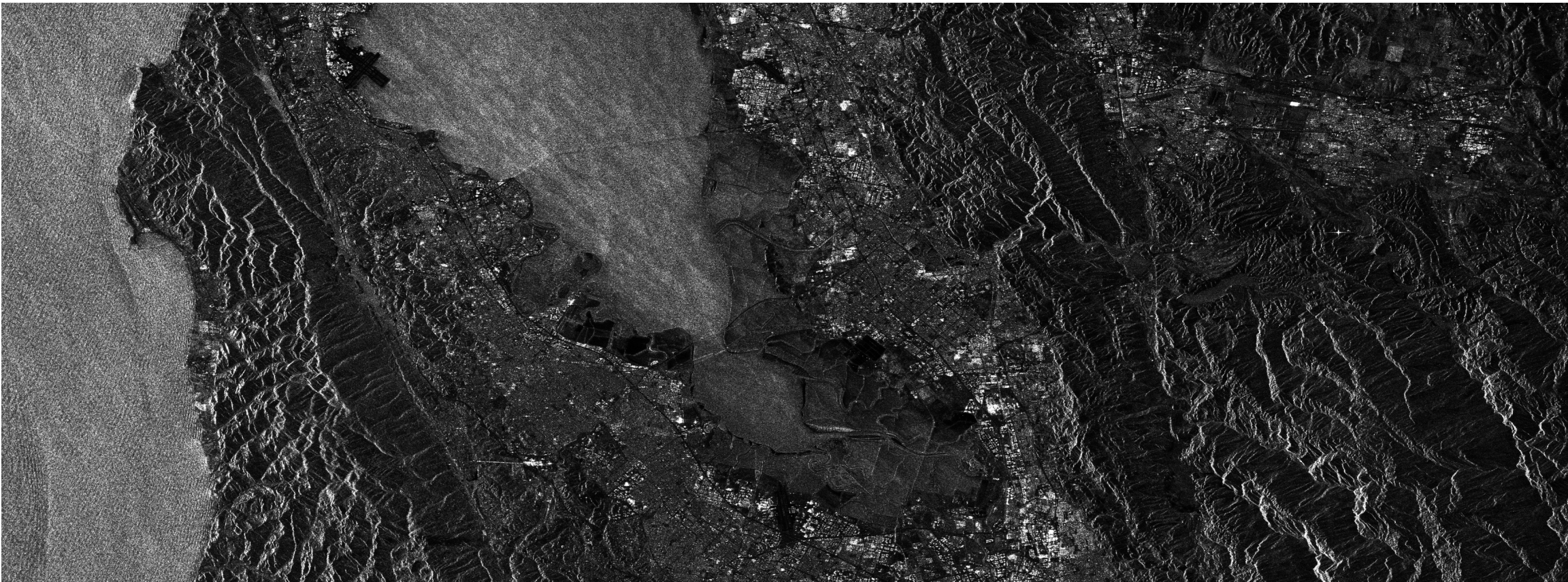
# Radar in remote sensing

- The increased use of radar in the remote sensing community is based upon several reasons.
  - The radar energy scatters of materials differently from optical energy, providing a complementary and sometimes better discrimination of surface features than optical sensors.
  - A radar carries its own illumination, so it works equally well in darkness.
  - The electromagnetic waves of common radar frequencies pass through clouds and precipitation easily.
  - Geometric resolution is independent of wavelength and little dependent on sensor geometry.

# Optical imagery over the San Francisco bay area



# SAR imagery over the San Francisco bay area



# Scattering mechanisms

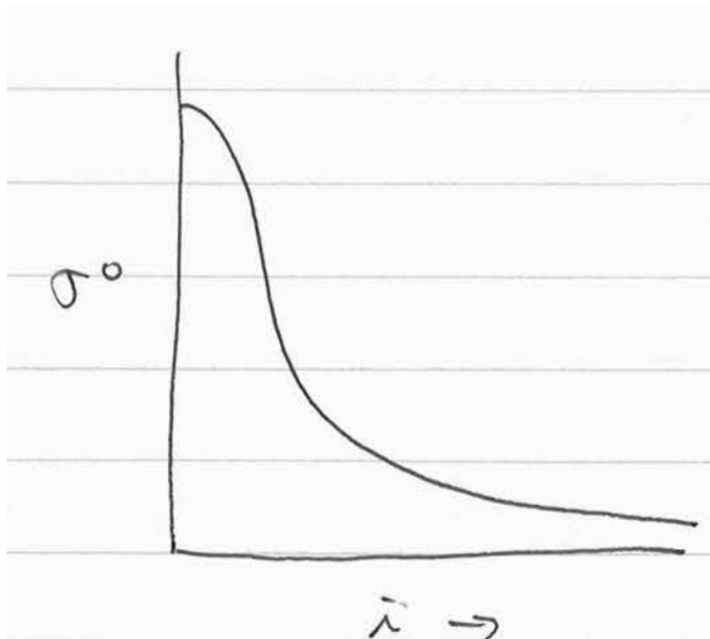
- We express “brightness” in a radar image in terms of the normalized radar cross-section,  $\sigma^0$ .
- The Radar Equation:

$$SNR = \frac{P_t G_t A_r A_{scat} \sigma^0}{(4\pi R^2)^2 k T_{sys} B}$$

- $\sigma^0$  embodies properties of the scattering surface itself and of the imaging geometry. Decoupling both effects is required if we want to interpret the apparent brightness in the images.

# Scattering mechanisms

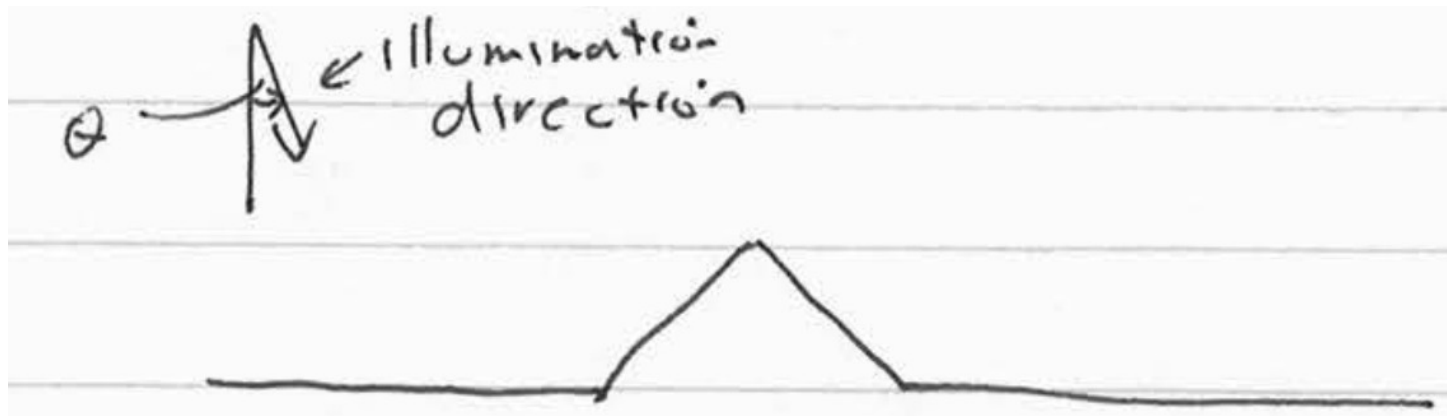
- The scattering phenomenology is dependent on the incidence angle  $i$ . In most cases, the incidence angle does not equal to the look angle.
- If we plot a typical curve of  $\sigma^0$  vs.  $i$ , we get something like this:



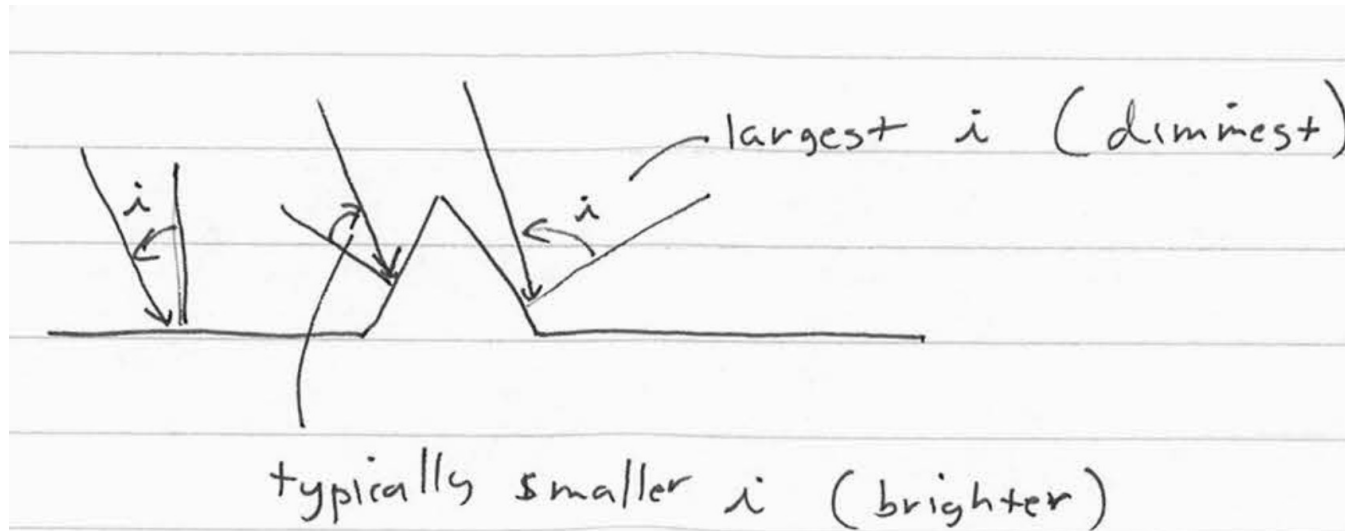
The scattering process can be viewed as letting more energy escape in the near forward direction than near backward.

# Slope modulation and topography

- To image the following surface



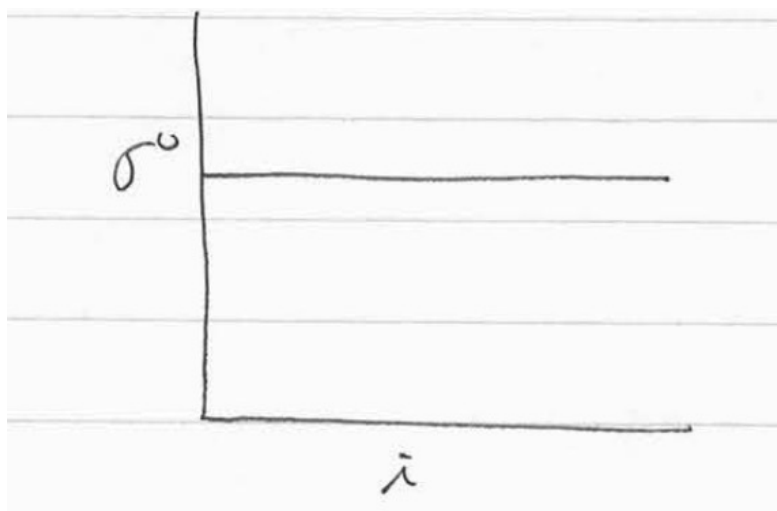
- Let's determine the local incidence angles:



# Slope modulation and topography

- Thus, this topographic feature would appear brighter on its near side and dimmer on its far side. This effect causes even subtle changes in topography to be visible in a radar image.
- Sensitivity to topography decreases as the wavelength decreases. At very short wavelengths,  $\sigma^0$  looks like:

This happens at optical wavelengths.



## Kilauea caldera, Hawaii

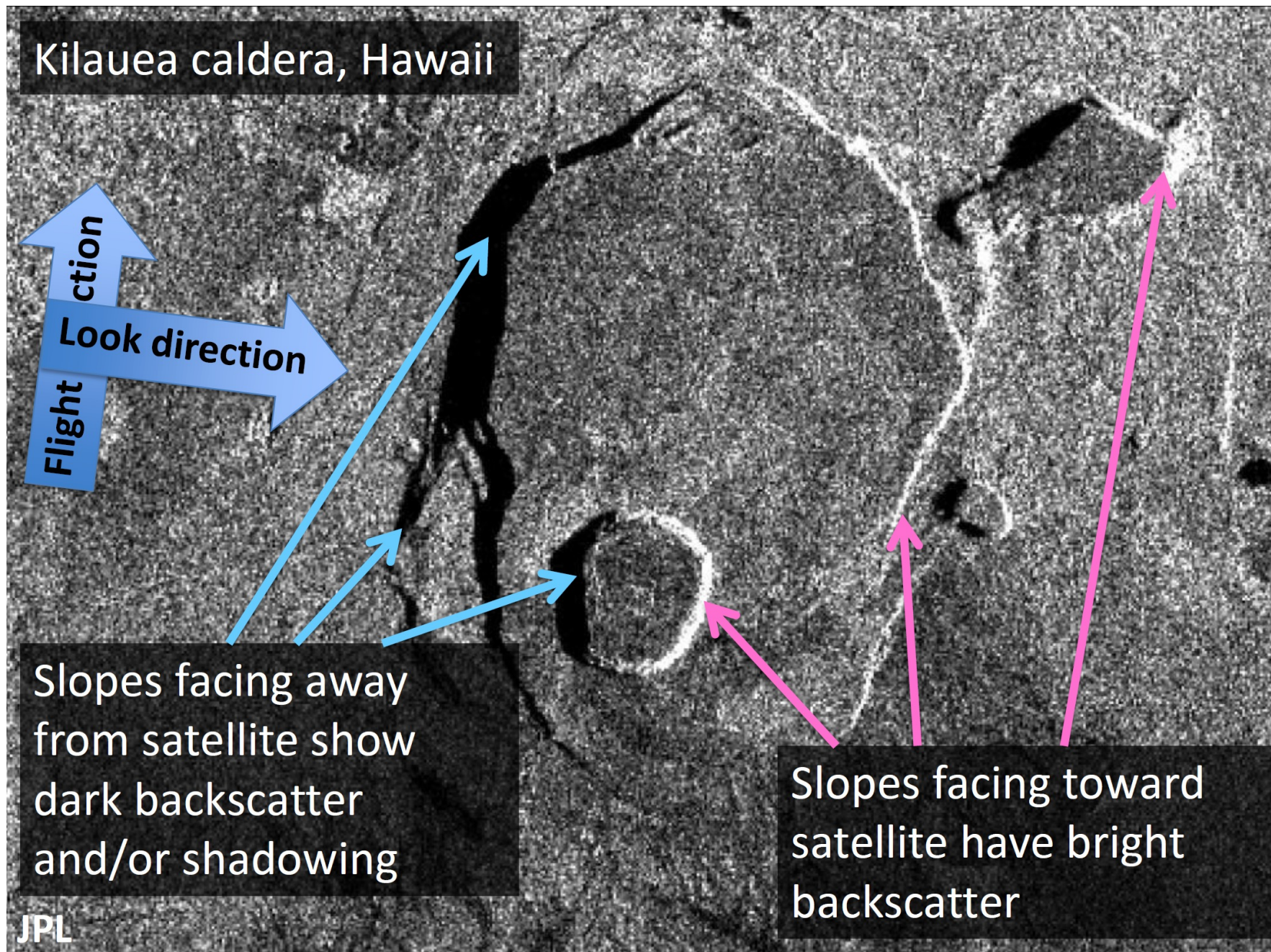
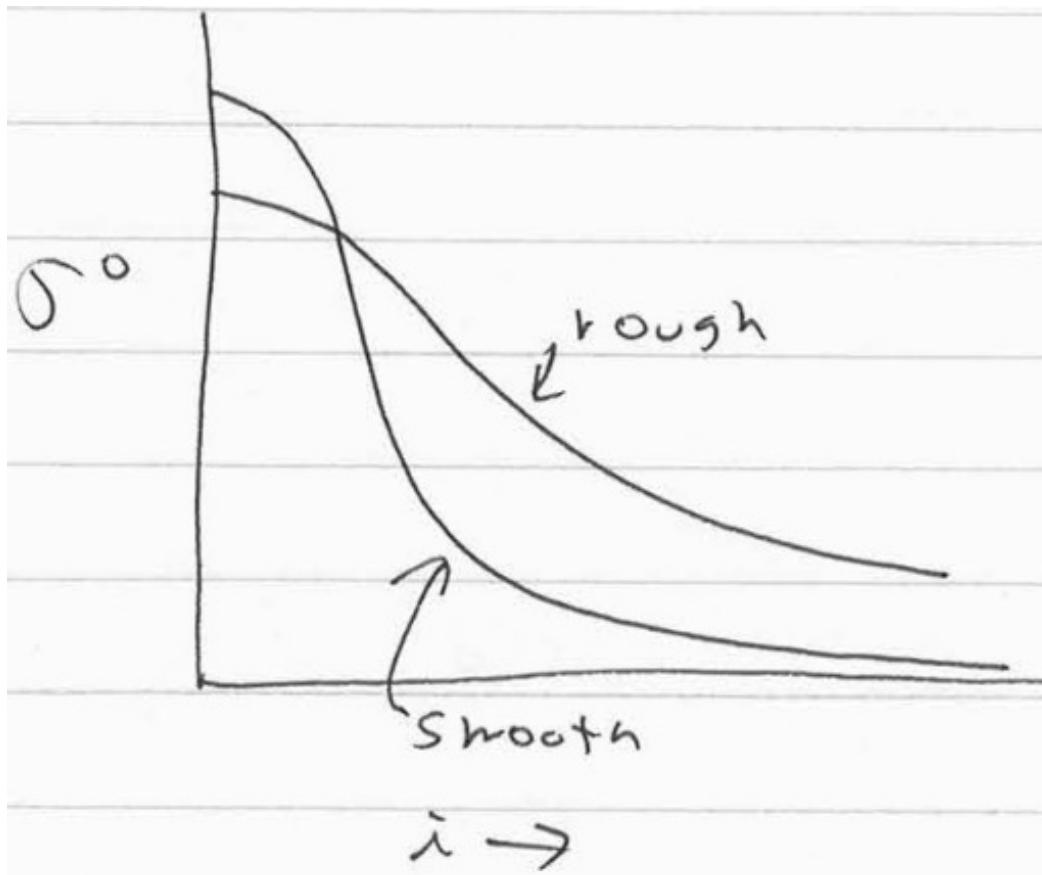


Image courtesy G. Funning

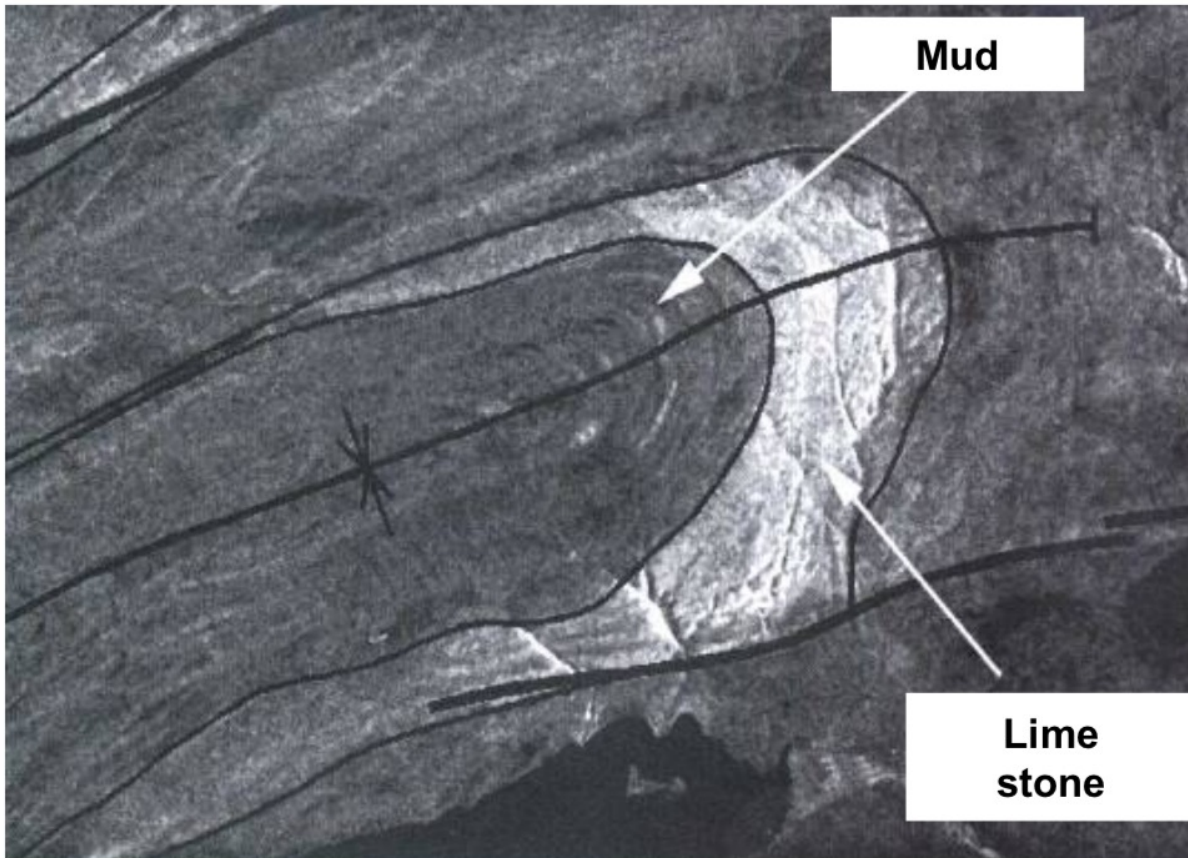
# Surface roughness variation

- So smooth and rough surface  $\sigma^0$  curve might look like:



Since topographic contrast depends on  $\frac{\partial \sigma^0(i)}{\partial i}$ , more shading is apparent in smoother areas than rougher areas.

# Effect of surface roughness



RADARSAT  
(C band, HH, 45°)

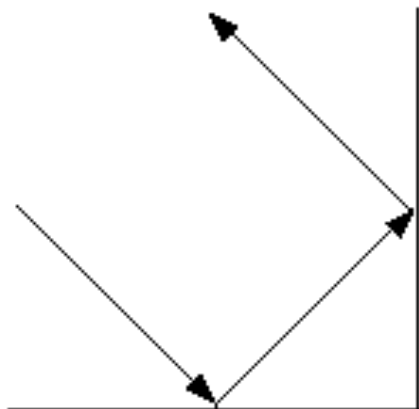
Quaternary lithology:  
Bathurst Island, Canada

From : RADARSAT Geology Handbook

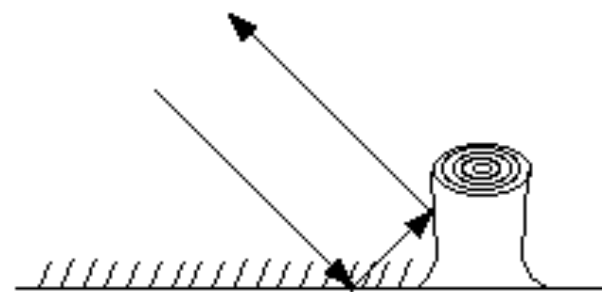
Mud fragments (smooth surface)  
→ low radar backscatter

Limestone → Higher backscatter  
because of rougher surface

# Scattering mechanisms

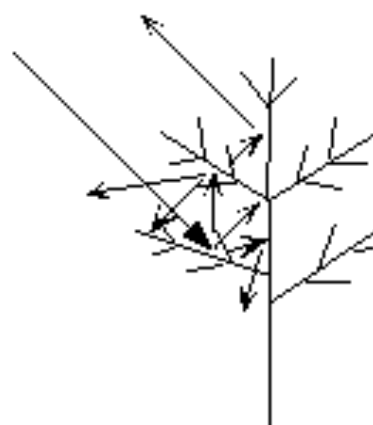


**Double Bounce**  
(Corner Reflector)

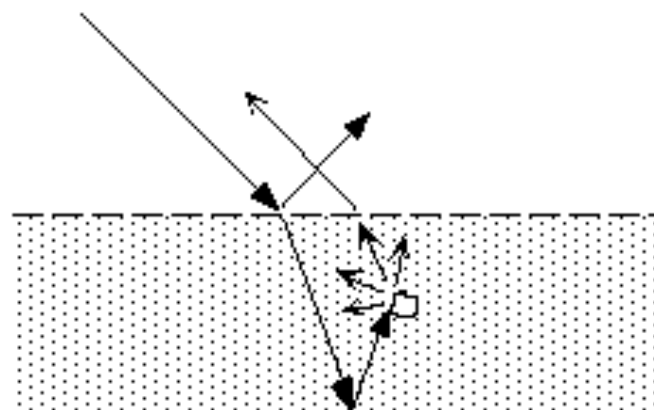


**Double Bounce**

One possible natural occurrence – reflecting off two smooth surfaces, grass and a freshly-cut tree's stump



**Volumetric Scattering**  
Example scattering in a tree

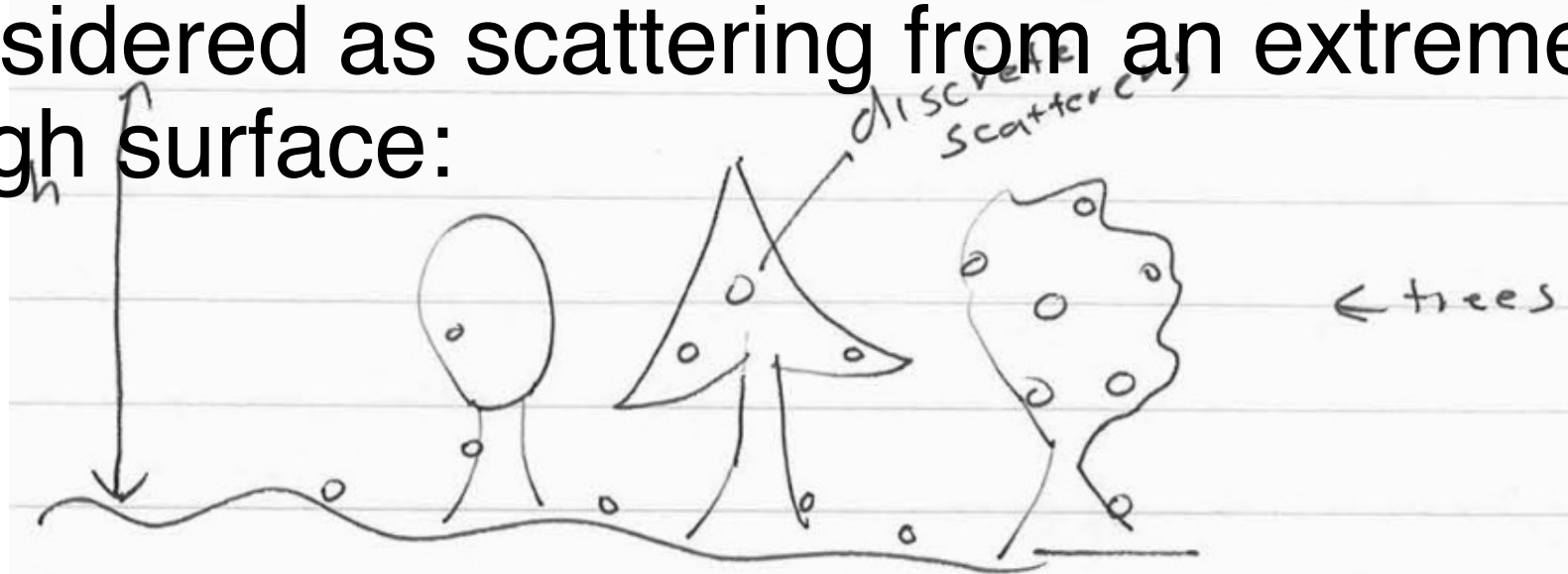


**Volumetric Scattering**

In this example the incident radiation is both reflected and refracted/transmitted through a layer of dry snow. The refracted radiation then reflects off underlying ice, scatters off a chunk of ice in the snow, and finally refracts back toward the receiver.

# Vegetation

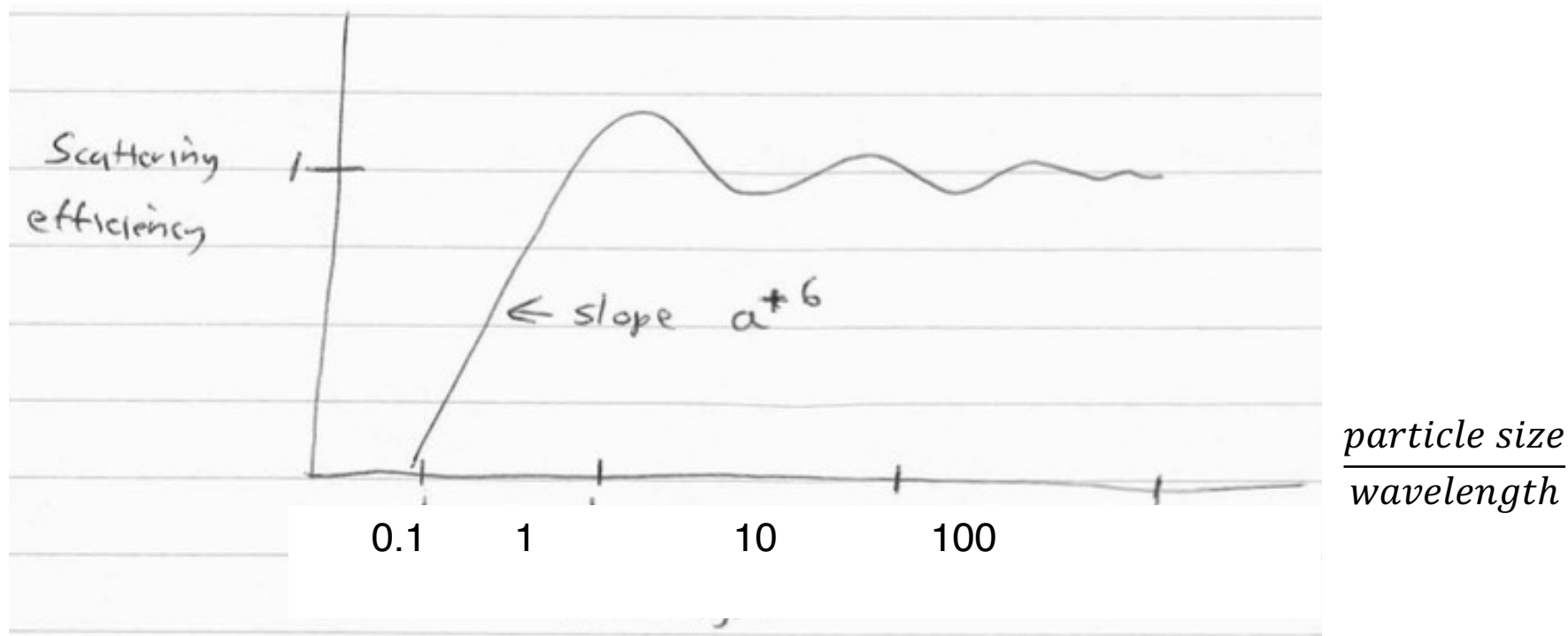
- Scattering from vegetation can be considered as scattering from an extremely rough surface:



These scatters are widely distributed in a very large volume. Hence we would expect little dependence on the incidence angle in very dense canopies when little or no energy penetrates to the ground. The sigma-zero vs. i curve is essentially flat in this case. Thus, one common method to calibrate radars without having to calculate incidence angle effects is to image a dense canopy such as Amazon rain forest.

# Wavelength dependence of backscatter

- Extinction/scattering cross section curves



We interpret this curve as implying that the effective cross-section of a particle is equal to its physical cross-section if the particle size is comparable to a wavelength or larger. In other words, the radar instrument is not very sensitive to sub-wavelength size particles.

# Wavelength dependence of backscatter

- We often state that radar backscatter is dominated by structures similar in size to the radar wavelength. Thus the use of multiple-wavelength radars permits investigation of a range of surface scatterer sizes.
- Incidentally, this is why the radar can see through clouds. The ice and water droplets in a cloud are much smaller than radar wavelength, but are large compared to optical wavelength.

# Vegetation canopy characterization

- Multiple wavelength radar can probe several aspects of a surface at once.

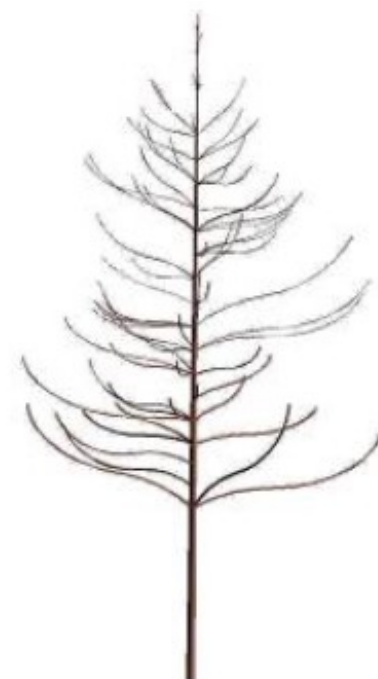


**Austrian pine**

**X band**  
 $\lambda = 3 \text{ cm}$



**L band**  
 $\lambda = 27 \text{ cm}$

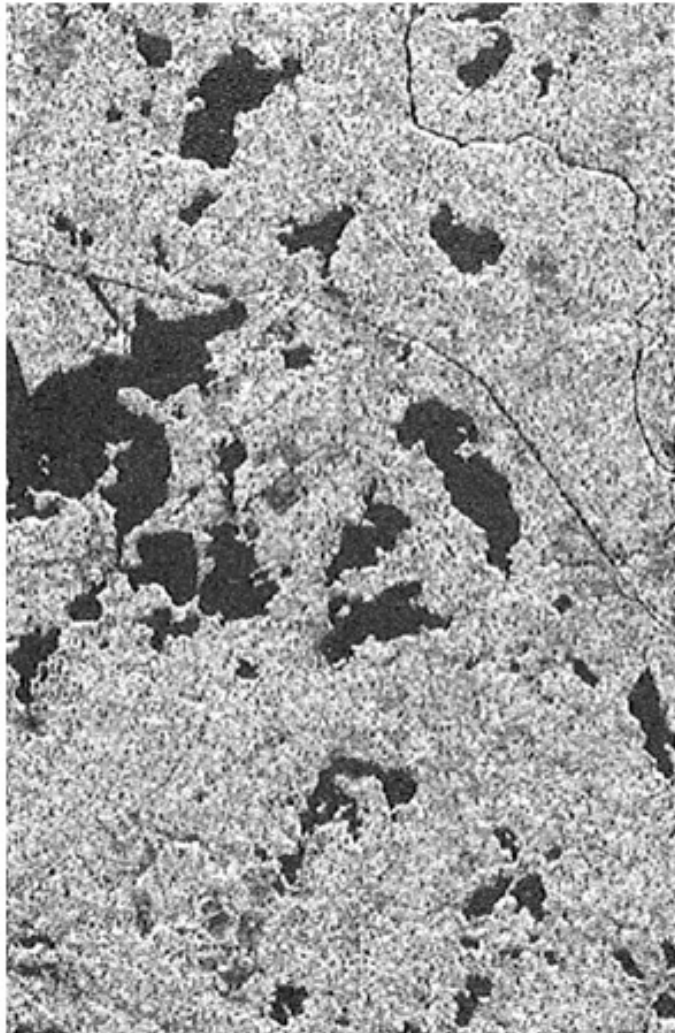


**P band**  
 $\lambda = 70 \text{ cm}$

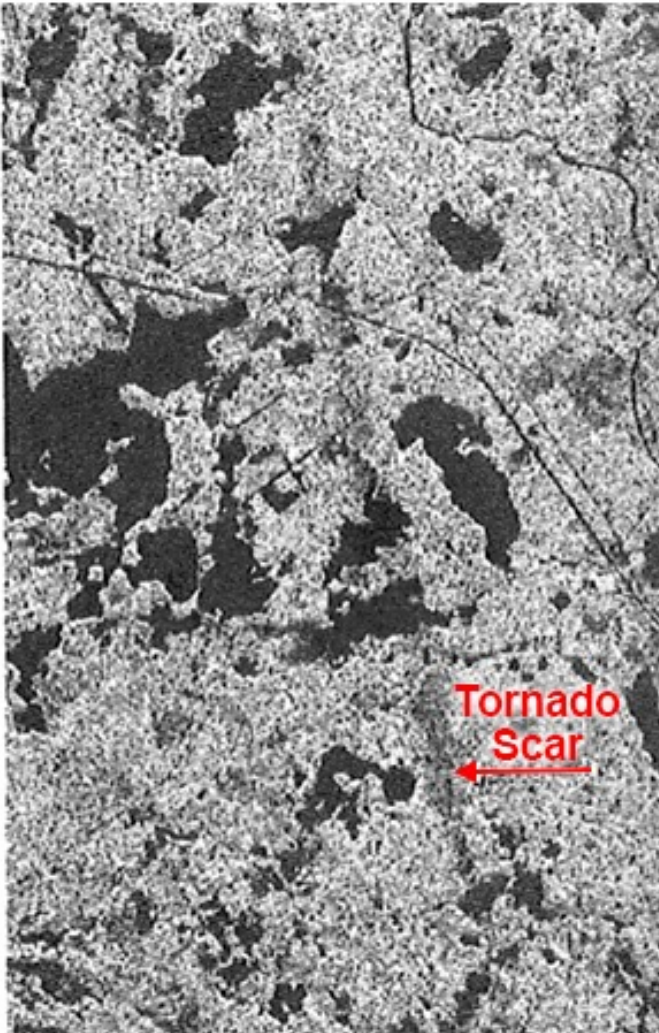


**VHF**  
 $\lambda > 3 \text{ m}$

# Vegetation Response to C-band and L-band Radar over Forrest area



**C Band (6 cm)**

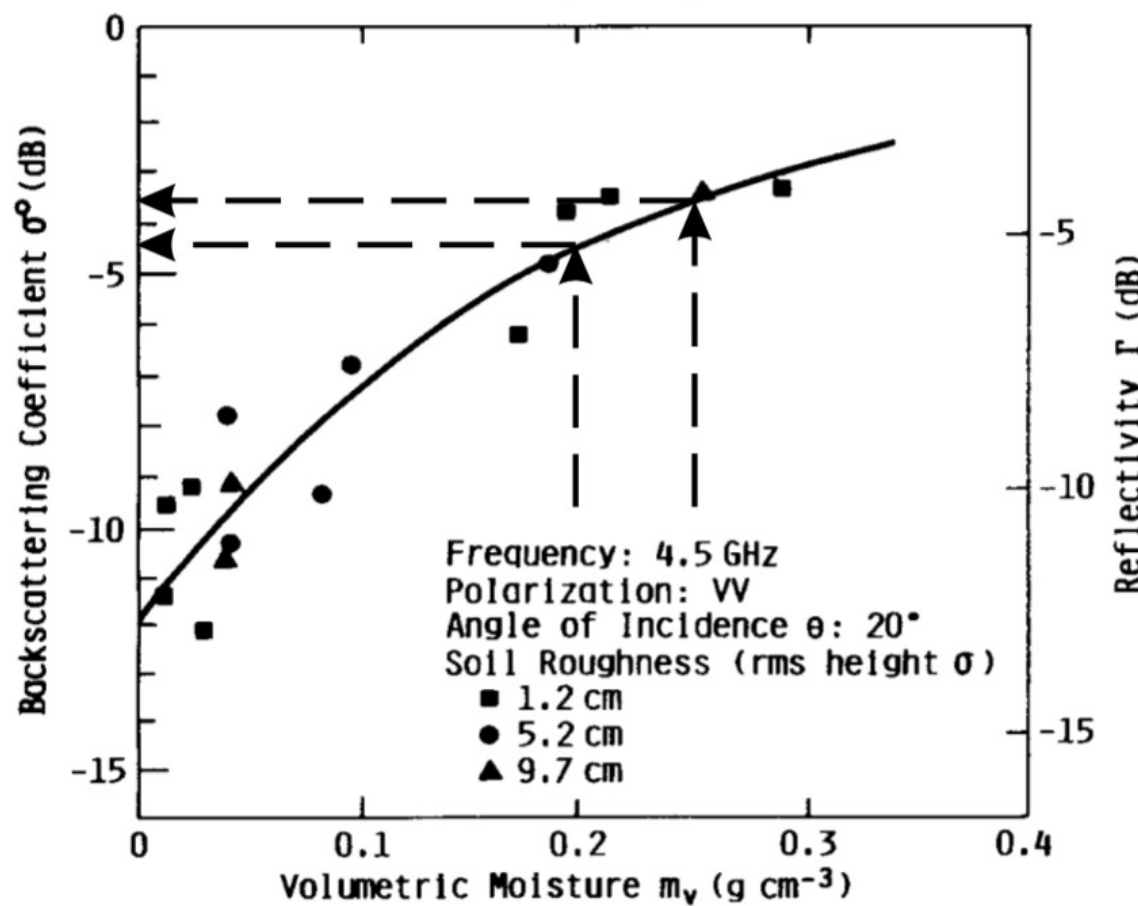


**L Band (24 cm)**

\* A tornado passed through the area approximately ten years prior to these images.

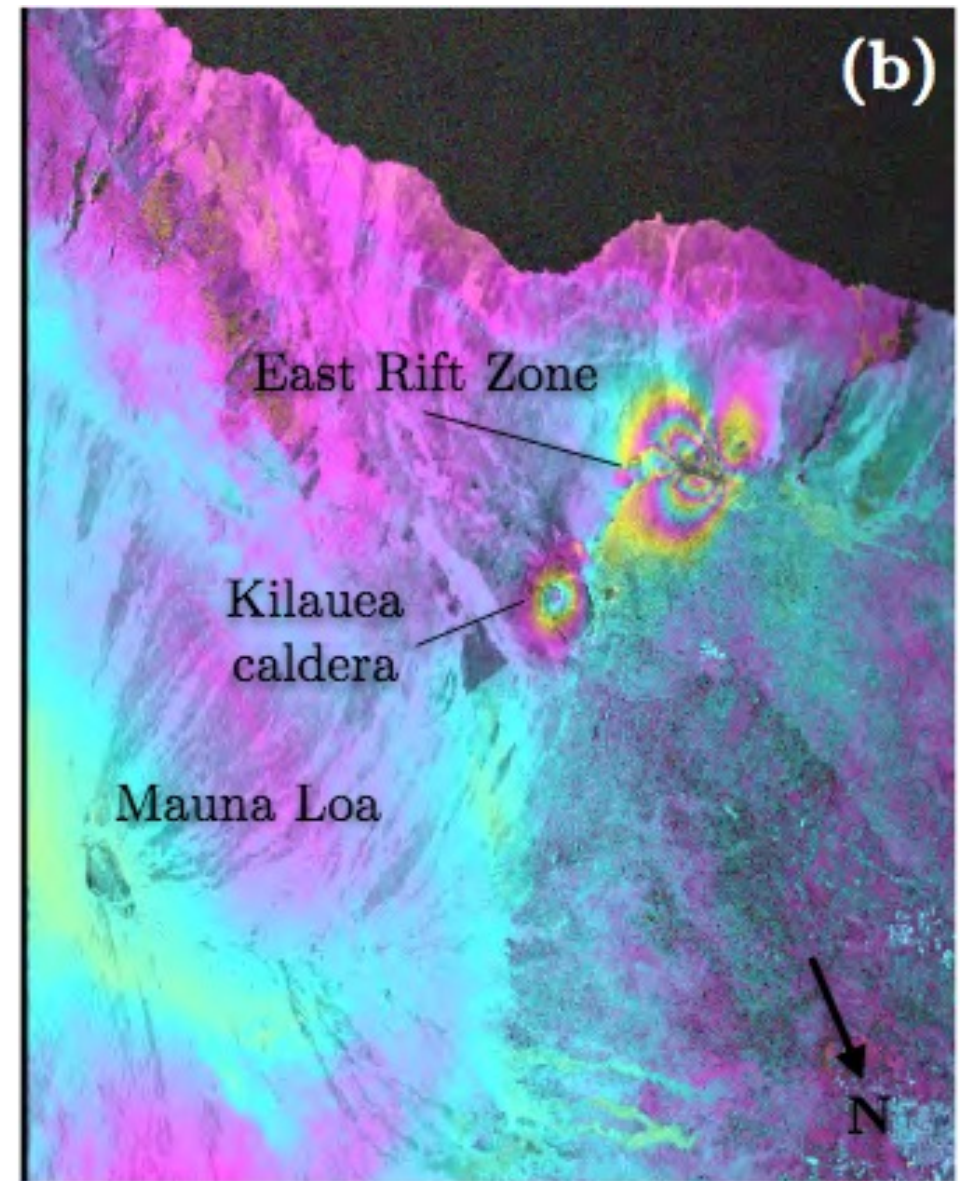
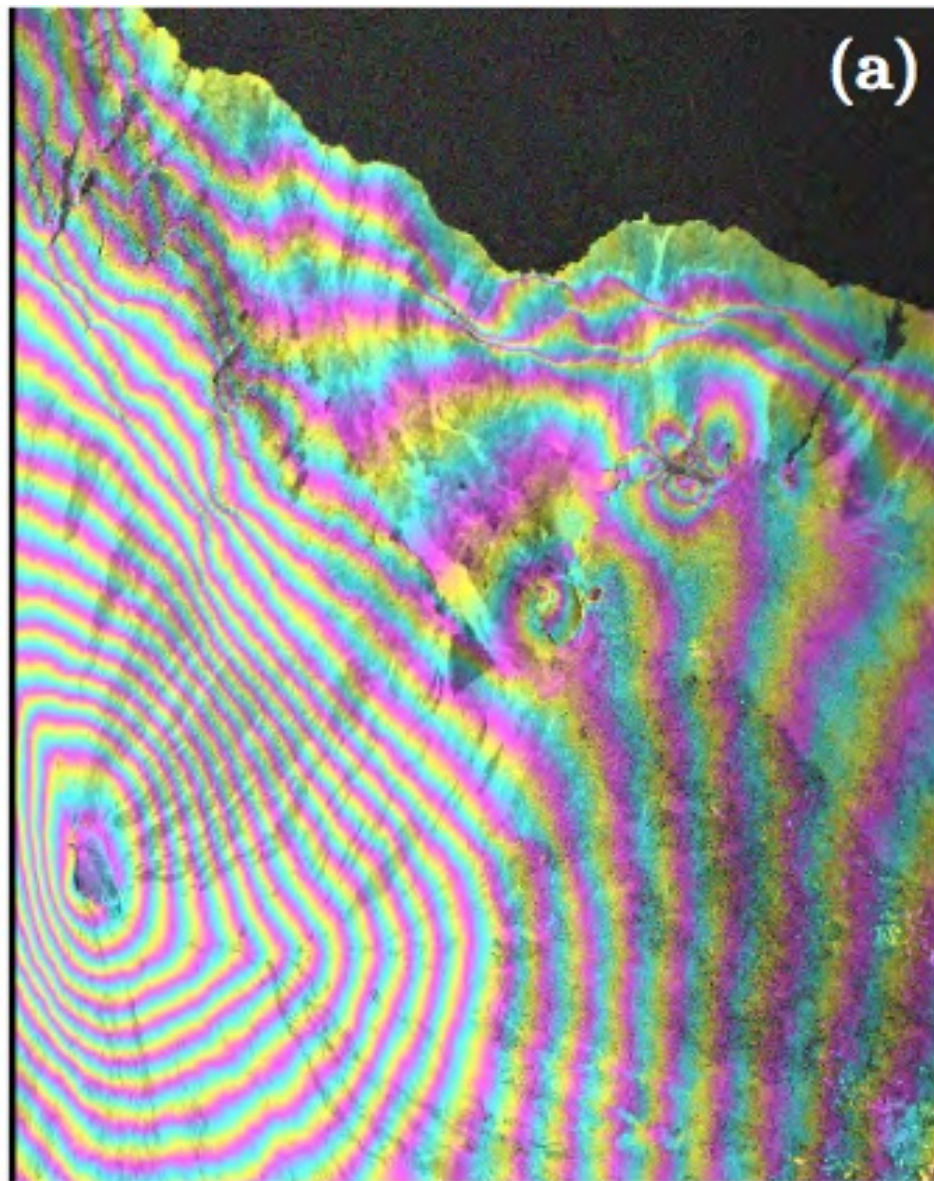
# Soil moisture

- Finally, the brightness depends greatly on composition through the dielectric constant of the scattering medium.



Adapted from Le Toan, T., 1982,  
"Active microwave signatures of soil  
and crops: Significant results of  
three years of experiments", In  
*Proceedings of International  
Geoscience and Remote Sensing  
Symposium (IGARSS 82)*

# InSAR for measuring surface topography and surface motion



# Technology for generation of DEM

- Optical-stereo instrumentation
  - Limited by cloud cover and lack of sunlight. Many areas of the globe are could-covered (e.g. high-relief or tropical areas) much of the time.
  - Require two cloud-free scenes with compatible imaging geometry.
  - Inhomogeneous quality and lack of consistency. As the DEM accuracy depends strongly on image feature contrast. Depending on the exact system, the spatial resolution of 1s-10s meters and vertical accuracies of 10s meters can be achieved. However, these accuracies cannot be achieved without suitable ground control point knowledge.
  - Truly global coverage is unlikely.

# Technology for generation of DEM

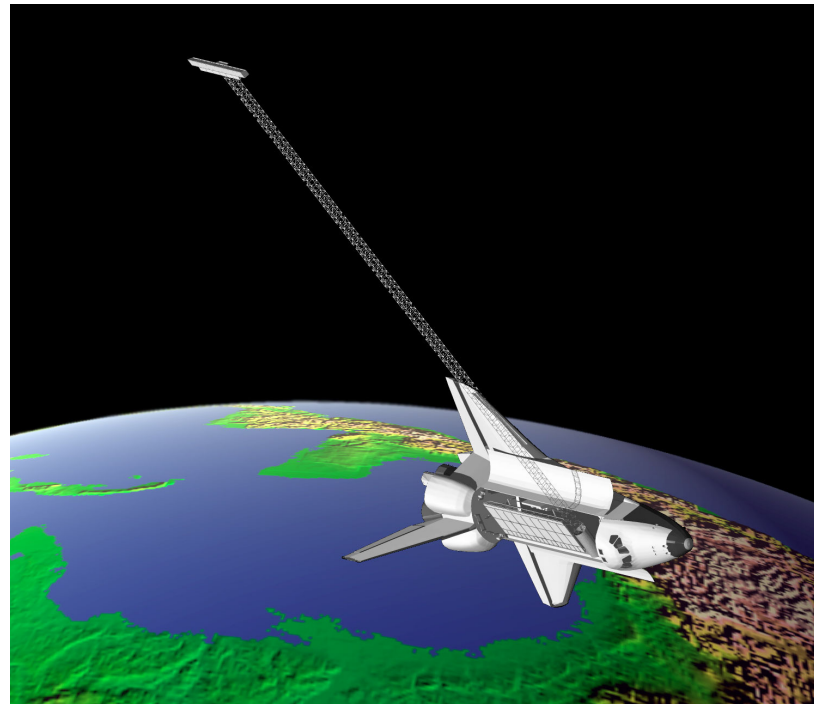
- Laser profiling instruments
  - Very high vertical accuracy ( $\sim 0.1\text{--}1$  meter).
  - The same atmospheric limitation noted for the stereo imaging affect laser performance.
  - A very narrow swath may be acquired at one time.  
For example, a 30-bean laser with each beam separated by 30 m leads to a swath of less than 1 km.
  - Laser altimeter's high vertical precision and low spatial coverage is ideal for certain studies such as polar ice volume measurements.

# Technology for generation of DEM

- Radar interferometry
  - Not limited by cloud coverage (Most severe storms may affect the radar systems with very short wavelength but this is much more rare than clouds in the sky).
  - Achieved required resolutions and accuracies in a reasonable mission life time. It is feasible to acquire “near-synoptic” global data in 6 months.
  - Reasonable cost

# Implementation options

- A single spacecraft with two displaced antennas
- Two spacecraft, each with a synthetic aperture radar, flying in formation to form the interferometer baseline.



The Shuttle Radar Topography Mission



TanDEM-X (TerraSAR-X add-on for Digital Elevation Measurement)

# SAR & InSAR applications



Imaging crustal deformation due to earthquakes

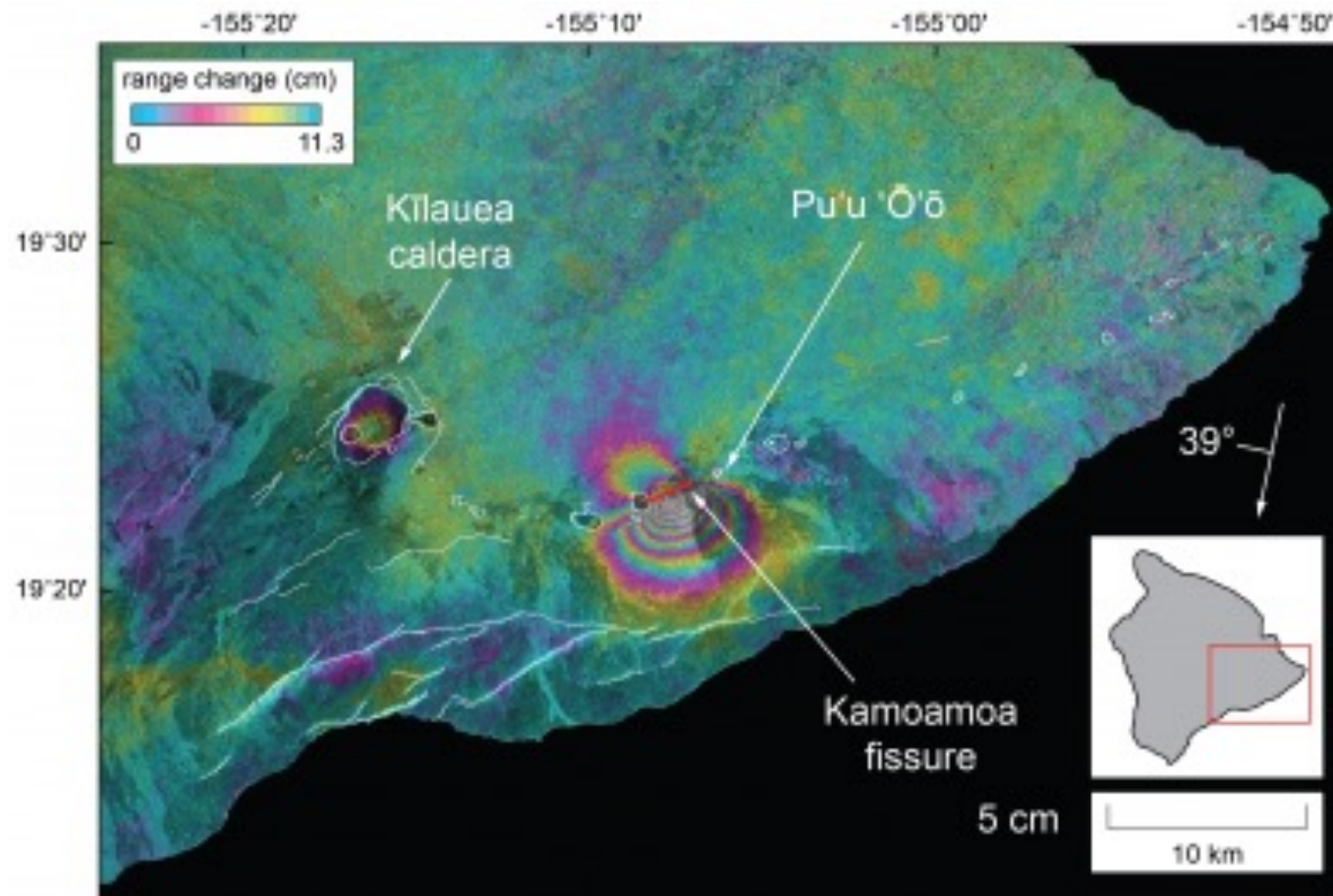
*The image covers a 90-by-110 km area from April 24 to August 7, 1992.*

*One color cycle represents 28 mm of deformation in Radar Line-Of-Sight (LOS) direction.*

[Massonnet et al., 1993]

# SAR & InSAR applications

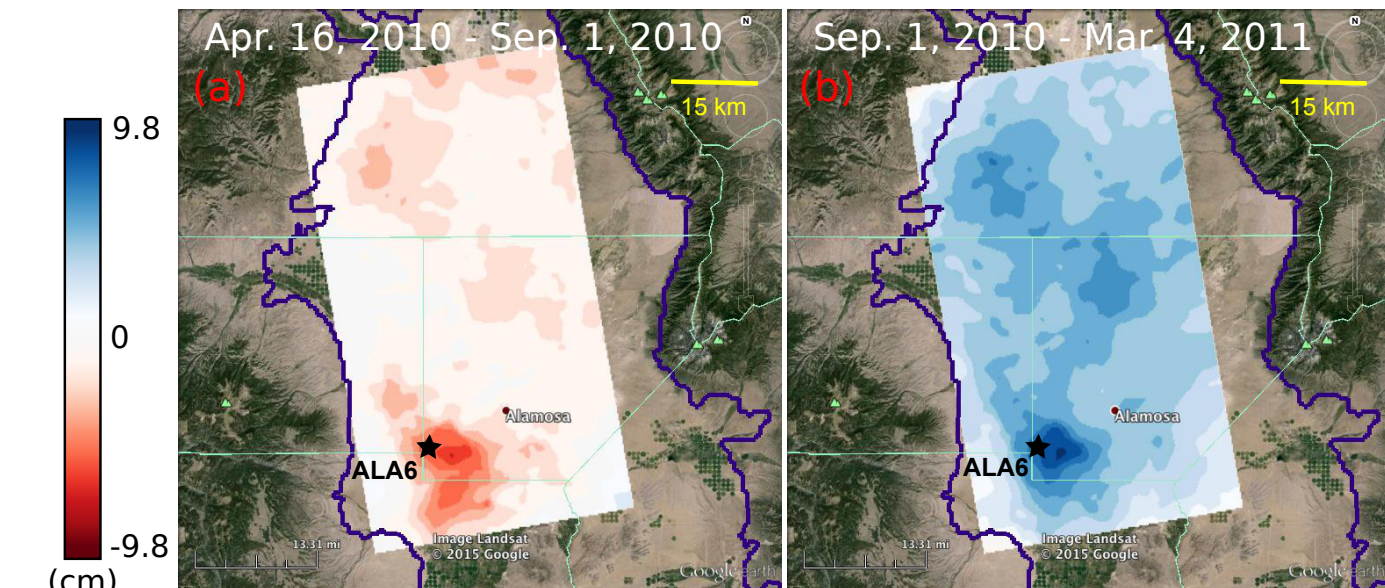
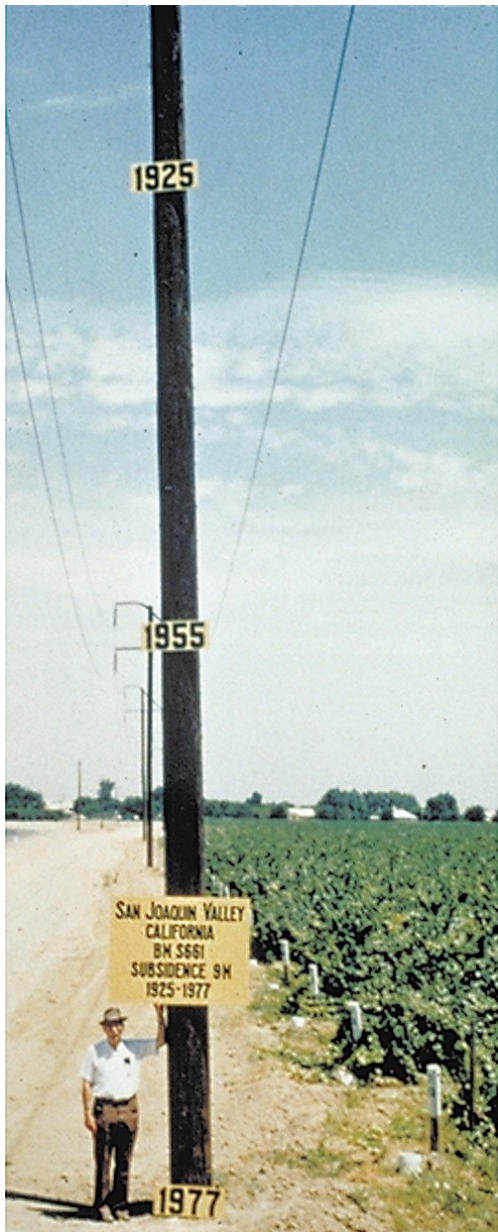
## Imaging surface deformation due to volcanic activities



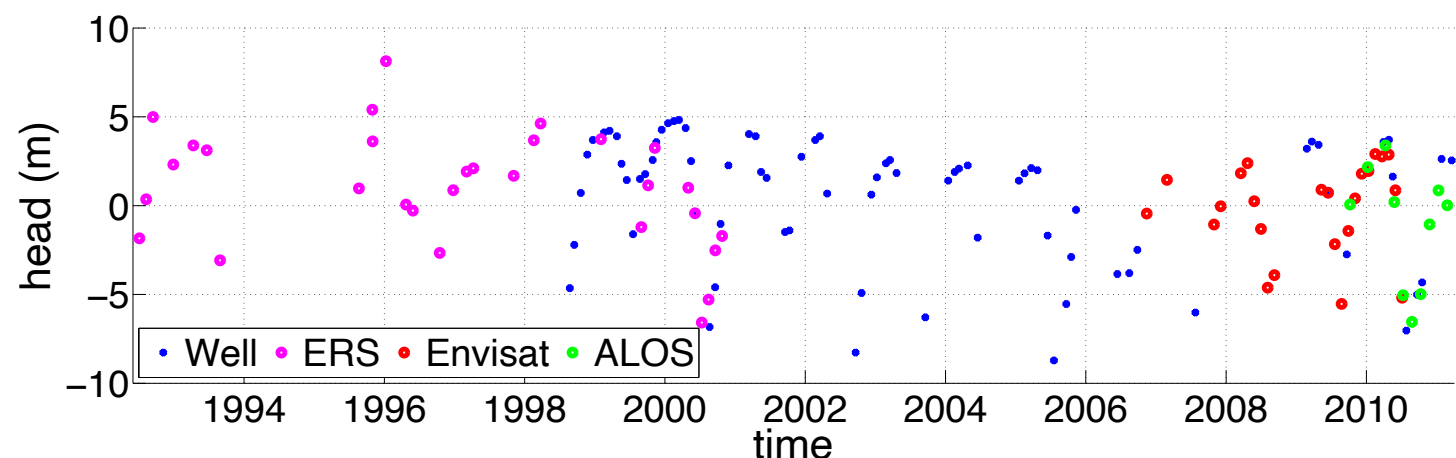
InSAR image Kīlauea, Hawai'i, March 2011 shows ground surface deflation at the summit caldera and inflation along the East Rift Zone (ERZ). Lava drained from the summit to ERZ and erupted at Kamoamoa.

[Image credit: USGS]

# SAR & InSAR applications



Ground deformation patterns associated with seasonal changes in head over  
San Luis Valley, CO

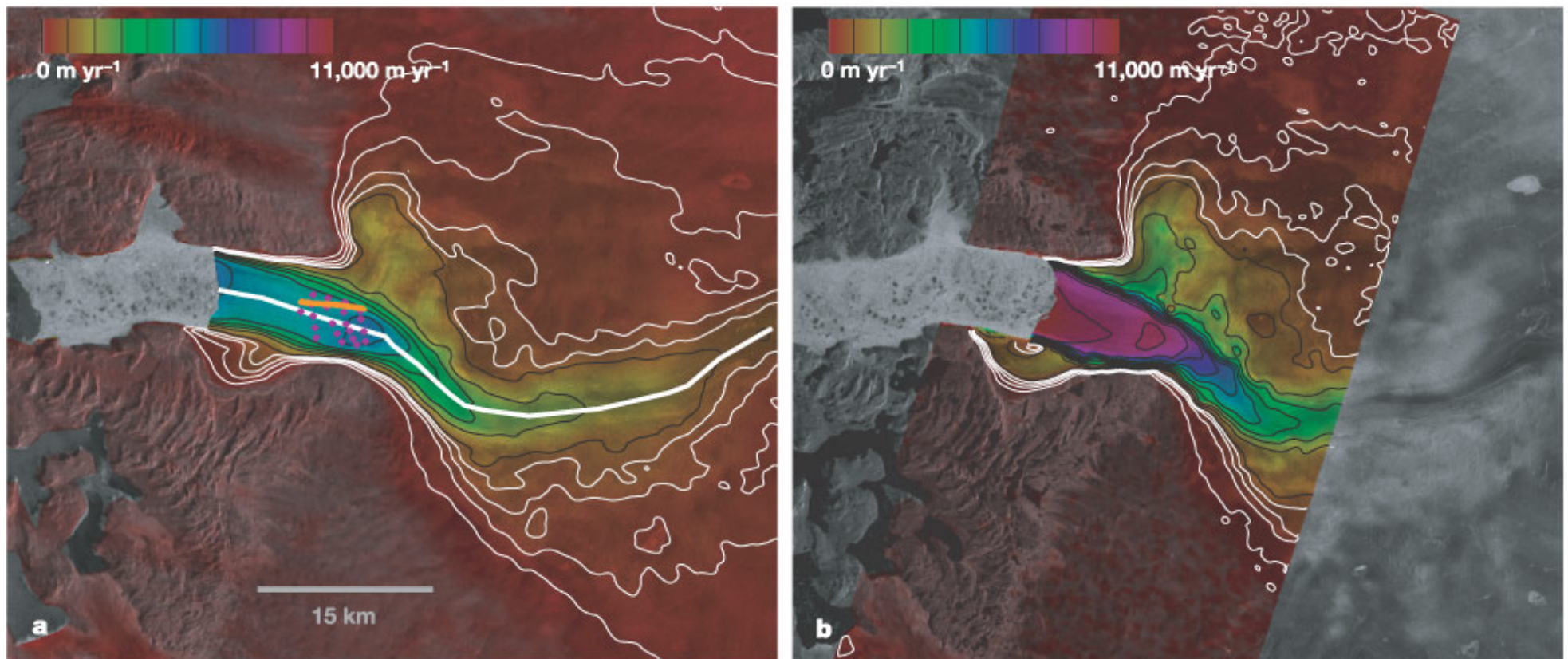


InSAR estimated groundwater levels at a confined aquifer well

[Chen, et al., 2016 & 2017]

# SAR & InSAR applications

Measure the motion of glaciers

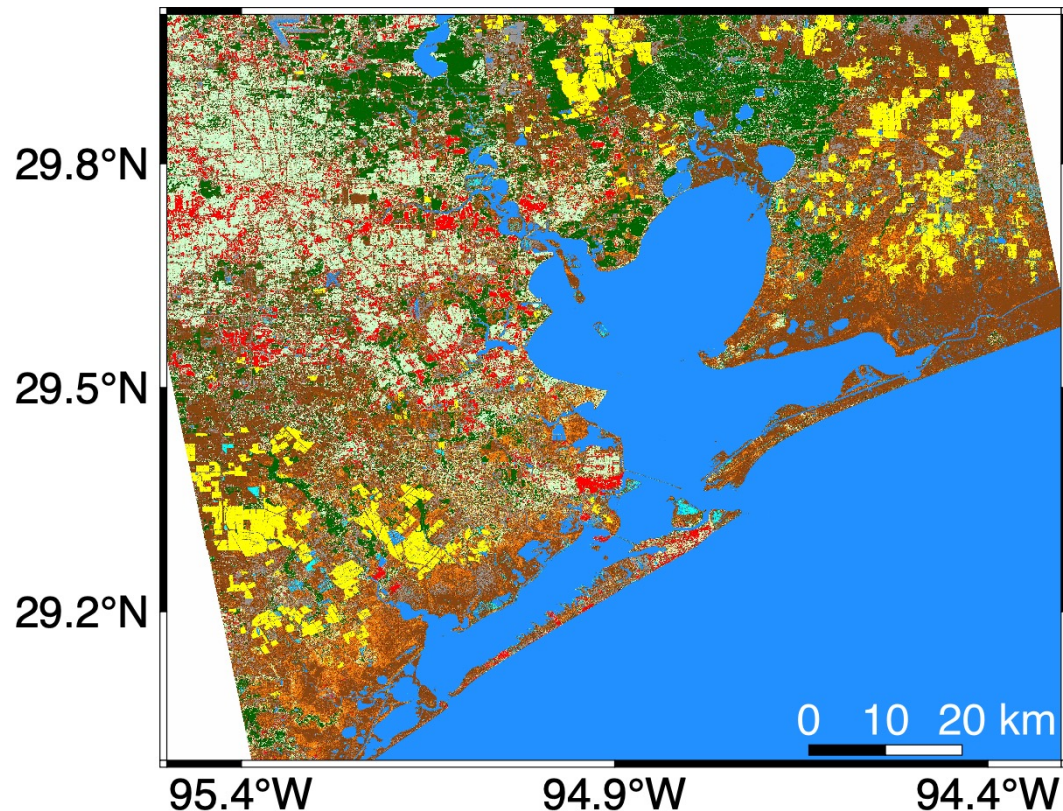


Ice-flow speed as colour over SAR amplitude imagery of Jakobshavn Isbræ in February 1992 (a) and October 2000 (b)

[Joughin, et al., 2004]

# SAR & InSAR applications

## Land Cover Classification for storm surge modeling



- Input features at each pixel:
  - Average SAR Amplitude
  - Average InSAR Phase Correlation
  - InSAR Phase Decorrelation Rate
  - Maximum SAR Amplitude
  - Minimum SAR Amplitude
  - SAR Amplitude Variation
  - DEM

[Wang, et al., 2021]

Open land types with different vegetation density

Water Mixed Urban Urban Forest